Impact of climate change on agricultural productivity and food security in the Himalayas: A case study in Nepal

D. Bocchiola[a,*], L. Brunetti[a], A. Soncini[a], F. Polinelli[b], M. Gianinetto[b]

[a] *Dept. Civil and Environmental Engineering ICA, Politecnico di Milano, Politecnico di Milano, L. Da Vinci, 32, 20133, Milano, Italy*
[b] *Dept. Architecture Built Environment and Construction Engineering ABC, Politecnico di Milano, G. Ponzio, 31, 20133 Milano, Italy*

The paradigmatic Dudh Koshi basin laid at the toe of Mt. Everest is largely visited by tourists every year, and yet agricultural productivity and food security therein are at stake under climate change. Agricultural yield in the area recently decreased, and the question arose whether cropping at higher altitudes may help adaptation. We investigated here the present, and future (until 2100) patterns of productivity of three main rain-fed crops in the catchment (wheat *Triticum L.*, rice *Oryza L.*, and maize *Zea Mais L.*). We explored food security using a nutritional index, given by the ratio of the caloric content from our target cereals, to daily caloric demand. We preliminary investigated whether vertical extension of the cropped area may increase food security. We did so by (i) mapping crops area using remote sensing, (ii) setting up the agronomic model *Poly-Crop*, (iii) feeding *Poly-Crop* with downscaled outputs from global climate models, and (iv) projecting vertical land occupation for cropping, po-pulation projections, and nutritional requirements. We estimated crop yield and food security at half century (2040–2050), and end of century (2090–2100), against a control run decade CR (2003−2013), under constant land use, and projected land occupation. On average, specific wheat yield would decrease against CR by −25%(rice −42%, maize −46%) at 2100, with largely yearly variability for unchanged land use scenario. Under modified land use scenario, wheat yield would decrease by −38%, while rice and maize yield would improve, maize very slightly (−22%, and −45%, against CR) in response to occupation of higher altitudes than now. Our food security index would decrease under all scenarios (111% in 2010, 49% on average at 2050, under a po-pulation peak, and 51% at 2100), and become more variable, however with potential for adaptation by colo-nization of higher lands (75%, 62%, at 2050, 2100). Very large expansion of one cereal (i.e. maize), may make food security more unstable, as mostly depending on erratic yield of that cereal only.

Keywords: Nepal, Himalaya, Food security, Crop yield, Climate change

1. Introduction

Food security worldwide is at risk under climate change, due to reduction of yield of key crops (Olesen and Bindi, 2002; Parry et al., 2004). Himalayas is especially at risk, given the complex topography, and social conditions therein (Malla, 2008; Ortiz et al., 2008; Bhatt et al., 2014). Also the present population growth in the area rise food demand (Strzepek and Boehlert, 2010). The most relevant crops here are cereals, especially wheat, *Triticum* L., rice *Oryza* L, and maize *Zea Mais* L (Supit et al., 2010). All these crops need rainfall, and possibly irrigation during growth season (Bocchiola et al., 2013; Nana et al., 2014; Bocchiola, 2015; Palazzoli et al., 2015). The impact of climate change on agriculture may include the effects of (i) rising CO_2 on respiration, mostly for *C3* plants (Morison, 1999; Leuning, 1995; Jarvis et al., 1999), (ii) changing temperature and rainfall, possibly leading to altered crop production along the XXI century (Brouwer, 1988; Rosenzweig and Hillel, 1998; FAO, 2009). The assessment report AR5 of the Intergovernmental Panel on Climate Change IPCC stated that negative impacts are more common than positive ones (IPCC, 2013), and that 5–200 M more people may be exposed to starvation until 2100 (Olesen and Bindi, 2002; Olesen et al., 2007; Schmidhuber and Tubiello, 2007). This study focuses on the Dudh Koshi river basin of Nepal. Nepal is very vulnerable to climate change (Awasthi et al., 2002; Matthews and Pilbeam, 2005; Rai, 2007; Eriksson et al., 2009a; Nyaupanea and Chhetrib, 2009; Maskey et al., 2011; Shrestha and Aryal, 2011; Karki and Gurung, 2012; Agarwal et al., 2014; Devkota and Gyawali, 2015; Palazzoli et al., 2015), and it has low adaptive capacity (Dulal et al., 2010). Small scale (~0.7 ha) subsistence agriculture is a backbone of Nepal's economy, with 78% work force, and contributes ~36% of Nepal's GDP (World Bank, 2012). With cropland

Received 3 April 2018;
Received in revised form 18 December 2018;
Accepted 20 January 2019

* Corresponding author.
E-mail address: daniele.bocchiola@polimi.it (D. Bocchiola).

Published Journal Article available at https://doi.org/10.1016/j.agsy.2019.01.008

only irrigated for 27%, above all in Terai (along Nepal-India border), arable land is largely rain-fed. Effects of global warming in Nepal include temperature increase (Rupa Kumar et al., 2006; Malla, 2008; Eriksson et al., 2009b), erratic rainfall, shorter winter, more frequent and longer droughts (Sharma and Dahal, 2010), and the question arises whether climate change will (negatively) impact cropping, and food security (Bocchiola, 2017). One needs tools to model crop production, to develop (i) potential adaptation to climate change, (ii) modified cropping strategies, and irrigation, and (iii) optimization of crop yield, and water usage.

The Koshi (Sapt Koshi) river (including Dudh Koshi studied here) is paradigmatic of the present situation of Nepal, i.e. with colonization of high altitude areas for cropping under the forcing of increasing population, and climate change (Gautam et al., 2003; Paudel et al., 2016a, 2016b). Population in the Dudh Koshi catchment as of 2010 can be estimated into ca. 190.000 persons, and expected to rise to ca. 280.000 at 2050, with slight decrease to ca. 230.000 at 2100, with a much higher density at the lowest altitudes. Recent studies (e.g. Neupane et al., 2013) showed large water-wise vulnerability of the area under climate change, and population increase. Our work here has shown that the cropping area increased from ca. 132 km^2 in the early 70's to ca. 284 km^2 now (Polinelli, 2017). The objectives of this study were (i) to simulate of crop yield (wheat, rice, maize) within the Dudh Koshi catchment, based on climate inputs, and the available agronomic information, (ii) to assess the potential effect of prospective climate change scenarios (until 2100) on crop production as per altitude distribution within the catchment, and (iii) preliminary assess the potential for adaptation by lifting of cropping area to higher altitudes.

To do so, we carried out an exercise as follows, (i) we tuned a spatially distributed, hydrologically based agronomic model *Poly-Crop* (Nana et al., 2014), able to mimic soil water budget, and crop growth, using daily weather data, (ii) we downloaded and properly downscaled climate scenarios (precipitation, temperature) until 2100, from 3 general circulation climate models (GCMs) from the IPCC fifth assessment report AR5 under three RCPs, 2.6,4.5,8.5, (iii) we fed the so obtained climate scenarios to *Poly-Crop* model, to obtain crop yield projections until 2100, (iv) we explored vertical variability of present and future crop yield in the catchment, (v) we projected some scenario of land use change for cropping, and we tested potentially improved food security therein.

In the Section "Region of investigation" we describe the Dudh Koshi basin, climate and agricultural setup therein, including preparation of crop maps. In the Section "Database" we describe the data base, including historical weather data, crop data, population, and nutrition data, which we used to define a *food security* index in the area. In the section "Methods" we report our methodology, including the *Poly-Crop* model, GCMs data handling, projections of crop yield, projections of cropped areas, and a correlation analysis against meteorological drivers. In the Section "Results" we provide the outputs of our modeling effort, and accuracy of the findings. In the Section "Discussion" we discuss our results, we provide a benchmark against available studies in the literature, and we deepen into potential for crop area expansion based on our findings, and present literature. We highlight limitations of the study, and outlooks. We then draw some conclusions, and outline possible future efforts.

2. Case study

The Dudh Koshi river (Fig. 1) is laid in the mid-hills of the central Nepal, located about 100 km East of Kathmandu (capital city of Nepal). It is one of the seven sub-basins of the Sapt Koshi (Savéan et al., 2015). Dudh Koshi is largely fed by snow and ice melt from the highest areas, including the Khumbu glacier, and it is undergoing reduction of stream flows in response to climate change, and glaciers' down wasting (Soncini et al., 2016).

Dudh Koshi river closed at Rabuwa Bazar has 90 km in length, and a catchment area of ca. 3600 km^2. One third of the basin is laid above 5000 m a.s.l. Some glaciers are present, mostly from 4800 to 6000 m a.s.l. Ice covered area is ca. 25% of total area. The climate ranges from subtropical to polar (Peel et al., 2007), and the topography is mostly rugged mountains, with occasional plateaus where farming is carried out. Dudh Koshi can be roughly split into three regions, (i) low, until 800 m a.s.l., covering ca. 23% of the catchment, of which ca. 38% used for agriculture, (ii) mid-Hills, 800–1800 m a.s.l., covering ca. 42%, and 15% with crops, and (iii) high-Hills, above 1800 m a.s.l. covering ca. 35% of the area, only 4% being cropped. Four precipitation seasons may be identified (e.g. Immerzeel et al., 2014), namely (i) pre-monsoon (March to May) with dry weather, and relatively high temperatures, (ii) monsoon, generally June to September, with ca. 80% of annual rainfall, (iii) post-monsoon (October to November), with little rainfall, and (iv) winter (December to February), generally dry with occasional precipitation from the westerlies. Agricultural area covers ca. 284 km^2, with wheat covering 30.6 km^2 (10.5%), rice 35.6 km^2 (12.5%) and a largest area with maize, of 219 km^2 (77%), the latter expanding recently for poultry. Maize in usually cultivated in battery with millet, *Panicum Miliaceum L.*, the latter sown before the former, in the same areas. Above 1800–2000 m a.s.l. however, they are no longer in battery, because of the cold temperature shortening the growing season, and instead they are grown in different areas. Reference values bring the areas of maize and millet with 80%, and 20% share respectively, and we therefore focus on the first one. Crop yield in central Nepal is largely dependent on seasonal weather patterns (Bartlett et al., 2011; WWF, 2012). Recent findings (WWF, 2012) for the Indrawati basin, ca. 100 km East of Koshi, indicated that water poverty index WPI (Cook et al., 2007) is ~52.5 out of 100 (i.e. medium poor), and access to water is a major issue, likely due to harsh topography and poor land use planning. The population of the area is therefore at large risk of severe impacts from changes in temperature and precipitation patterns (NAPA, 2010; WWF, 2012; Karki and Gurung, 2012). Among others, Bhatt et al. (2014) investigated crop yield (rice, maize and wheat) to climate change in the Koshi basin, finding significant effect temperature and precipitation in the growing season. However, in some high-elevation areas, positive impacts of warming were observed on rice and maize yields (see also Palazzoli et al., 2015). Accordingly, in the Dudh Koshi basin assessment of future crop productivity in response to climate change is necessary, aimed at designing adaptation strategies.

3. Database

3.1. Topography, land use, and soil data

Topography was extracted from a Digital Elevation Model (DEM) of the U.S. Geological Survey (U.S.G.S.), with resolution 30 × 30 m^2 (Hirano et al., 2003). Land use for cropping was assessed here for the purpose of the study. Initial classification of land use for cropping based on maps from ICIMOD (Kabir et al., 2015) provided some difference against Nepal wide statistics of land use as given by Ministry of Agricultural Development MOAD (2013a). Therefore, we developed a land use map for the area (Gianinetto et al., 2017), specifically for crop cover. A time series of images collected since 1975 (Landsat-1/MSS) to 2010 (Landsat-8/OLI) was classified with a rule-based expert system implemented with a decision tree algorithm, based on topography and NDVI. The classification scheme used a multi-temporal approach to map each crop in the growing season, and time of maximum vigor. The thematic maps so produced display consistent statistics against Nepal wide statistics. The observed dynamics of land cover changes is highly correlated with both demography, and climate data (see Table 1 for a resume of land cover). Land cover for 2010 was used as a spatial support for *Poly-Crop* model. A Curve Number *CN* map of the catchment (90 × 90 m^2) was built based on land use maps and the 'Soil and Terrain database for Nepal' from FAO (2004), and used to assess maximum soil water content S_{max} for *Poly-Crop*. Soil texture down to 1 m was

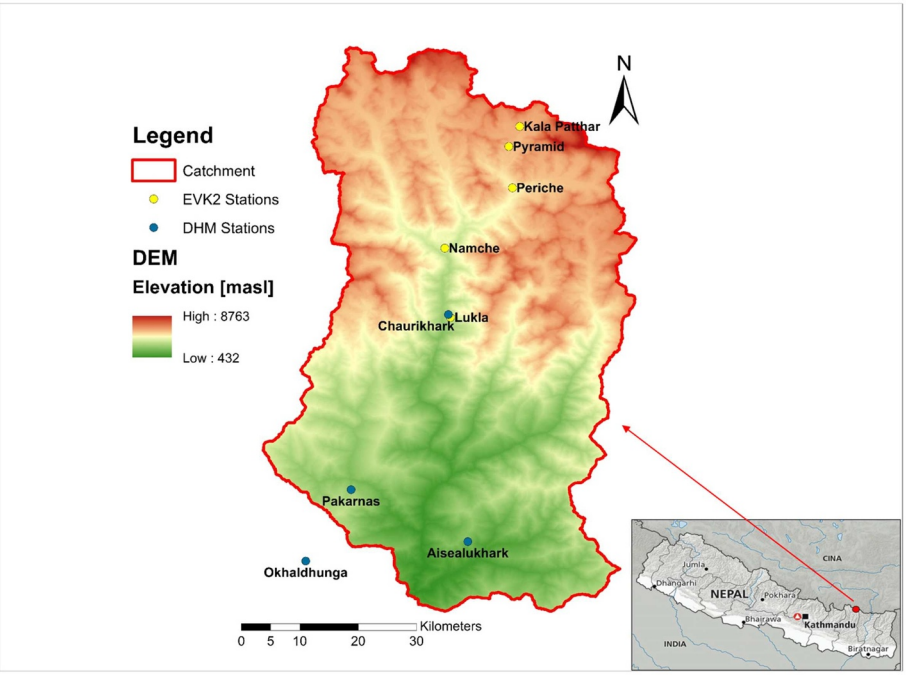

Fig. 1. Case study area. (a) Dudh Koshi basin location and elevation zones. Weather stations used in the study reported.

Table 1
Dudh Koshi catchment. Subdivision of land use in class, and crop types.

Land use/crops	Area [km^2]	Watershed Area [%]
Forest	1365.9	37.9%
Shrubland	179.0	5.0%
Grassland	517.9	14.4%
Barren area	429.5	11.9%
Water body	15.1	0.4%
Glaciers	864.1	24.0%
Built-up area	0.1	0.0%
Wheat	24.6	0.7%
Rice	17.4	0.5%
Maize	193.0	5.4%
Total	3606.5	–

defined according to Hengl et al. (2017), resulting into *sandy loam* (42% sand, 32% silt, 26% clay), which we used to define hydraulic soil properties (Table 3).

3.2. Meteorological data

Poly-Crop model uses daily precipitation, maximum and minimum temperature, and solar radiation. Meteorological data (Fig. 1) were collected from the Department of Hydrology and Meteorology of Nepal (DHM, 4 stations), and EVK2CNR association (5 stations). A resume of the stations is given in Table 2. Spatial distribution of meteorological inputs was pursued for distributed modeling. Temperature and precipitation were referred to an area of influence using Thyessen polygons, and then modified for altitude according to *lapse rates*. Yearly precipitation lapse rate was taken as from Salerno et al. (2015). This displays linear increase until 2500 m a.s.l. or so (+1.16 mm/m, $R^2 = 0.69$), and exponential decrease above that ($\sim e^{bAlt}$, with $b = -9{\cdot}10^{-4}\,m^{-1}$), typical of the Himalayas (Bookhagen and Burbank, 2010; Soncini et al., 2015, 2016). For crop modeling, an estimate of global radiation is necessary. This was inferred in each cell by calculation of theoretical (ephemeral) radiation R_t times a clear sky index *CSI* (ratio of real to theoretical radiation R/R_t), calculated daily at Pyramid station.

Table 2
Dudh Koshi catchment. Meteorological data used for *Poly-Crop* simulation. *T* is mean daily temperature, T_{min}, T_{max}, min/max daily temperature, *P* precipitation, *R* solar radiation.

StationID	Alt [m a.s.l.]	Period	Variable	Resolution raw data
Okhaldhunga	1720	1996–2013	T, T_{min}, T_{max}	Daily
Lukla	2231	2003–2013	T, T_{min}, T_{max}	hourly
Namche	3570	2003–2013	T, T_{min}, T_{max}, P	hourly
Periche	4260	2003–2013	T, T_{min}, T_{max}, P	hourly
Pyramid	5035	2003–2013	T, T_{min}, T_{max}, P, R	hourly
Aisealukhark	1924	1970–2013	P	daily
Pakarnas	2231	1970–2013	P	daily
Chaurikhark	2619	1970–2013	P	daily

3.3. Population, and nutritional data

To model and project land occupation for cropping, we used population data (ICIMOD, 2017), and nutrition standard in the area (NGMAD, 2012; FAO, 2016). Population data within the Dudh Koshi were available as per the three districts for the year 1991, 2001, and 2010. For 1975 we used Nepal population, and proportional sharing within each district. An estimate of consumed calories per day per person for Nepal was available for 1990, 2000, and 2010, which we used as a proxy for nutritional demand within the Dudh Koshi catchment. For 1975 a linear regression was used based on the three subsequent years. Agricultural yield for calculation of available food were taken from ICIMOD (2015), during 1981–2010 (as per the three districts). Reference caloric values of our three main cereals were also taken from literature.

4. Methods

4.1. Poly-Crop model

The spatially semi-distributed *Poly-Crop PC* model was used (Addimando et al., 2015; Nana et al., 2014; Bocchiola, 2015; Bocchiola and Soncini, 2017), including a simplified crop growth simulator, such

as *Cropsyst* (Stöckle et al., 2003), WARM, and WOFOST (Confalonieri et al., 2009). Only one soil layer was considered for simplicity. The hydrological model is based on water budget equations, giving soil water storage S [mm] at two time steps (t, $t + \Delta t$).

$$S^{t+\Delta t} = S^t + P\Delta t + I\Delta t + ET\Delta t - Q_g\Delta t - Q_s\Delta t. \quad (1)$$

Here at daily scale P is rainfall [mmd^{-1}], I is irrigation [mmd^{-1}] if available, ET [mmd^{-1}] is evapotranspiration, Q_g [mmd^{-1}] is groundwater discharge, and Q_s [mmd^{-1}] is overland flow (for soil saturation, i.e. when $S = S_{max}$). Daily biomass growth is the least of a water (transpiration) dependent growth (G_{TR}), and a solar radiation dependent growth (G_R)

$$G_{TR} = \frac{T_{eff}\ BTR}{VPD};\ G_R = L_{tbc}\ PAR\ f_{PAR}\ T_{lim} \quad (2)$$

with G_{TR} [kgm^{-2}day^{-1}] transpiration dependent biomass growth, T_{eff} [mday^{-1}] effective (actual) transpiration, VPD [kPa] vapor pressure deficit, BTR [kPakgm^{-3}] biomass transpiration coefficient, G_R [kgm^{-2}day^{-1}] radiation dependent growth, L_{tbc} [kgMJ^{-1}] light to biomass conversion coefficient, PAR [MJm^{-2}day^{-1}] photosyntetically active radiation, f_{PAR} [.] fraction of incident PAR intercepted by canopy, and T_{lim} temperature limitation factor [.]. Nutrients availability was assumed, and nitrogen budget was not assessed (i.e. N is not limiting). This is not generally true, but preliminary investigation indicated little need/use of manuring in the Koshi basin. Crop growth stages depend on thermal time (or degree-day) during the season (Stöckle and Nelson, 1999). On vegetated areas ET depends on the LAI, iteratively calculated in each day. ET depends on daily vegetation growth, and vegetative stage (Stöckle et al., 1994), as

$$f_{PAR} = 1 - exp(-k\ LAI_{cum}), \quad (3)$$

and

$$T_{eff} = 86400\ \frac{C}{1.5(\Psi_s - \Psi_x)}, \quad (4)$$

where k [.] is an extinction coefficient for solar radiation, LAI_{cum} [m^{2}m^{-2}] is the cumulated leaf area index until the day f_{PAR} is calculated, C [kgsm^{-4}] is root conductance, Ψ_s [Jkg^{-1}] is soil water potential, depending on water content (Campbell, 1985), Ψ_x [Jkg^{-1}] is leaf water potential, 86,400 is number of seconds per day, and 1.5 a factor to convert root conductance into hydraulic conductance. To model crop growth against CO_2 we used *CropSyst* model approach, namely (i) Monteith's (1977) approach, modifying G_R in Eq.(2), and (ii) Tanner and Sinclair (1983) approach, modifying G_{TR} in the same equation. Modified versions of these methods tuned against recent experiments are implemented in *Cropsyst* (Stöckle et al., 1992; Stöckle et al., 2003; O'Leary et al., 2015), and were adopted here as follows.

$$G_{R,CO_2} = G_R\ C_{R,CO_2} = G_R \frac{(-c/(350\ (1-c))\ CO_2\ c)}{(-c/(350\ (1-c))\ CO_2 + c)}$$
$$G_{TR,CO_2} = G_{TR}\ C_{TR,CO_2} = C_R/((\delta + (\gamma\ 336/300))$$
$$/(\delta + \gamma((36\,CO_2)/(350\,C_R) + 300)/300)), \quad (5)$$

with δ [kPa°C^{-1}] psychrometric constant, and γ [kPa°C^{-1}] slope of the saturated vapor pressure-temperature curve. The coefficient c depends upon crop type (*C3/C4*), i.e. upon fixation of carbon. When doubling CO_2 from 350 ppm to 700 ppm, *C3* plants (rice/wheat) rise potential biomass by 25% ca. ($c = 1.7$), while *C4* plants (maize) rise biomass no > 10% ($c = 1.21$, Tubiello et al., 2000).

For each crop management practices were specified, i.e. planting, and harvest and kill. All operations were scheduled based on a calendar gathered from available literature (e.g. Bhattarai et al., 2002; Sijapati et al., 2013; Palazzoli et al., 2015). For simplicity and lacking specific indication, one only harvest season was taken for each cereal. Only rain-fed agriculture was considered, as per the lack of irrigation reported. Harvest was carried out at maturity (using degree-day, Table 3). Manual tuning was pursued by trial-and-error approach, modifying the parameters highlighted in a sensitivity analysis, kept within a range from literature. Calibration was pursued against yield (2003–2013) data provided by MOAD (2013a), using mean yield.

4.2. Climate projections from GCMs

Three coupled GCM models were used here (Table 4), namely CCSM4 (Gent et al., 2011, https://www.earthsystemgrid.org), ECEarth (Hazeleger, 2011, http://ecearth.knmi.nl/) and ECHAM6 (Stevens, 2013, http://cera-www.dkrz.de). Here, three RCPs adopted in the IPCC's Fifth Assessment Report AR5 (IPCC, 2013, RCP 2.6, 4.5, 8.5) were used. Daily precipitation was downscaled by a Stochastic Space Random Cascade (SSRC) approach (e.g. Bocchiola and Rosso, 2006; Bocchiola, 2007), so being usable for unbiased development of climatic projections (see Groppelli et al., 2011a, 2011b). Model calibration was carried out during the control period CR (2003–2013) with observed daily precipitation series (corrected for snowfall at the highest altitudes). GCMs' precipitation was downscaled to each of the precipitation stations, and subsequently redistributed against altitude according to *lapse rates*. Downscaling of temperatures is made by comparison of mean seasonal temperatures at the local stations, against mean values from GCMs. The difference (ΔT) between average values is used to correct future temperatures.

4.3. Crop yield projections

Using the tuned *Poly-Crop* model, fed with weather inputs from the three considered GCMs (and three RCPs), we simulated potential basin wide crop yield of wheat, rice, maize, for two reference decades (11 years for consistence with control period CR, 2003–2013), namely 2040–2050 (hereon, 2050), and 2090–2100 (hereon, 2100). So doing, we obtained nine potential scenarios of crop yield. The climate input and concentration of CO_2 were set according to values estimated by each model and each RCP, and land use until 2100 was projected as reported below.

4.4. Projected agricultural cover

To evaluate the future development of the agricultural system, we applied a simplified model. First, we calculated the elevation distribution of each crop during the reference period (years 1975, 1990, 2000, 2010). Elevation belts where chosen with a 500 m vertical jump, large enough to filter noise deriving from image classification (e.g. clouds, etc.), and still representative of the vertical patterns of crop cover. We investigated the link between nutritional per capita per day requirement in the catchment C_n [Cald^{-1}p^{-1}], function of the year as reported above (C_n = 1940–2544 Cald^{-1}p^{-1} during 1975–2010), and the nutritional power available within the catchment C_a [Cald^{-1}p^{-1}], which is a function of crop yield (on average during 1975–2010, 1.73, 2.42, and 2.16 tonha^{-1}, for wheat, rice, and maize respectively), and nutritional power of each (~3390, 1300, and 3650 Calkg^{-1}, respectively).

$$C_a = \frac{1}{365 N_p} \sum_{c=1}^{3} A_c Y_c P_c, \quad (6)$$

with N_p population, c crop index, A_c [km^2], Y_c [Ton] and P_c [CalTon^{-1}], area, yield and caloric power of crop c. Here N_p is taken as the population of Solukhumbu and Kotang (as per the ratio of the district included within the Dudh Koshi area, ca. 30%) districts. The underlying hypothesis is that land occupation occurs in response to food demand from the local population, satisfied also (but not only) by cereal consumption. Accordingly, a direct proportionality should hold between C_n and C_a, meaning that a main driver of land colonization for cropping is indeed population growth. We defined a nutritional index, i.e. the ratio between availability and demand of energy (food) within the

Table 3
Dudh Koshi catchment. *Poly-Crop* model parameters (*calibration), and crop (sowing date) for Dudh Koshi basin.

Par.	Definition	Unit	Range	Wheat	Rice	Maize
θ_w	Soil water content wilting	[−]	–	0.15	0.15	0.15
θ_L	Soil Water content limit	[−]	–	0.28	0.28	0.28
θ_S	Soil Water content saturation	[−]	–	0.48	0.48	0.48
T_{base} [a]	Base temperature	[°C]	0 ÷ 15	6	10	8
T_{cutoff} [a]	Cutoff temperature	[°C]	0 ÷ 45	30	35	30
T_{opt} [a]	Optimal temperature	[°C]	$T_{base} \div T_{cutoff}$	18	25	25
d-sow	Sowing date	[Julian]	–	305	135	74
GD_{emerg} [a]	Emergence degree-day	[°C-day]	0 ÷ 500	150	80	52
GD_{flow}	Flowering degree-day	[°C-day]	$GD_{emerg} \div 1500$	1600	850	820
GD_{mat} [a]	Maturing degree-day	[°C-day]	1000 ÷ 2500	3000	1400	1800
GD_{harv} [a]	Harvest degree-day	[°C-day]	–	500	130	200
GD_{max_root}	Max root depth degree-day	[°C-day]	–	900	970	950
GD_{leaf} [a]	Leaf duration degree-day	[°C-day]	$GD_{emerg} \div GD_{mat}$	1000	600	830
R_{d_max} [a]	Max root depth	[m]	0.1 ÷ 3.0	0.75	0.85	1
K_{c0}	ET coltural coefficient	[−]	0.1 ÷ 1.6	1.1	1.05	1.2
LtBC	Light-biomass conversion	[g MJ^{-1}]	1 ÷ 5	3	3	4
U_{max}	Max watering day	[kg m^{-2} day^{-1}]	5 ÷ 15	13	11	12
$\psi_{x,sc}$	Xilematic potential critical	[J kg^{-1}]	−3000 ÷ −500	−1600	−1200	−1200
$\psi_{x,w}$	Xilematic potential wilting	[J kg^{-1}]	−3000 ÷ −1100	−2200	−1800	−1800
Dr	Dryness factor	[kPa^{-1}]	–	0.02	0.03	0.02
BTR	Trasspiration-biomass conversion	[kPa kg m^{-3}]	3.5 ÷ 8.5	4.5	5.5	8
SLA	Specific leaf area	[m^2 kg^{-1}]	20 ÷ 60	20	27	24
ls	Stem-leaf partition	[m^2 kg^{-1}]	1.5 ÷ 4	4	2.4	2.6
k	Solar radiation ext.	[−]	0.3 ÷ 0.8	0.5	0.5	0.4
HI	Harveest index	[−]	0 ÷ 1	0.52	0.3	0.5
Alb	Albedo	[−]	0.1 ÷ 0.3	0.2	0.2	0.27
T-thresh	Transpiration threshold	[−]	0 ÷ 1	0.5	0.6	0.6

[a] Parameters used for calibration.

Table 4
Main properties of the GCM models used here.

Model	Research Centre	Grid size[°]	n. cells	layers
CCSM4	Nat. Center for Atmospheric Research, USA	1.25° × 1.25°	288 × 144	26
EC-Earth	Europe-wide consortium, EU	1.125° × 1.125°	320 × 160	62
ECHAM6	Max Planck Institute for Meteorology, GER	1.875° × 1.875°	192 × 96	47

catchment, namely.

$$C_{\%} = \frac{C_n}{C_d}. \tag{7}$$

We then studied the relationship between the share of area within any given altitude belt that was occupied by each crop in each of the four chosen years, and the corresponding number of inhabitants in that year. We used simple linear equations to project forward vertical land occupation for cropping on the basis of the projected population. Here preliminarily we neglected the effects of potential climate drivers on land use change. Preliminary assessment pursued by Gianinetto et al. (2017) indicated that demographic, and socioeconomic pressure is mostly driving the colonization of high altitude areas, and that climatic and topographic drivers basically provide limitations (see also Paudel et al., 2016a, 2016b). Accordingly, we considered population as the main (only) driver in this preliminary analysis. We pursued a preliminary analysis by setting a maximum value for slope above which cropping is thought as unfeasible (i.e. 25°, e.g. Paudel et al., 2016a), and we verified that the crop areas (i.e. the sum of area for each of our three cereals) expected in the future according to our projections would always be smaller than the available areas within each of the covered altitude belts, i.e. that extension of cropped areas would be possible.

4.5. Correlation analysis against meteorological drivers

To interpret the potential effect of climate variables on crop yield under the large uncertainty entailed in future projections, a correlation analysis was carried out. Specifically, yearly values of Y (CR, 2050 – 3 RCPs – 3 GCMs, 2100 – 3 RCPs – 3 GCMs) were correlated against CO_2 (constant within decades), temperature during growth season T_g, and precipitation in the same season P_g. A preliminary analysis indicated that seasonal values of T and P influenced differently cropping behavior, so we pursued this analysis seasonally. For winter wheat we considered two trimesters after sowing date, namely NDJ, and FMA. For summer rice and maize, we used AMJ and JAS.

5. Results

5.1. Crop yield from Poly-Crop model

A summary of calibration results of the model is reported in Fig. 2, and Table 5. Fig. 2 displays simulated crop yield for wheat Y_w, rice Y_r, and maize Y_m, against values reported by MOAD (2013a) for Solukhumbu and Kotang district. Average temperature T, and precipitation P during growth season are also reported, split in trimesters (wheat, NDJ, FMA, rice/maize AMJ, JAS). Total crop area of the Koshi catchment here is laid for ca. 60% within Solukhumbu district, and for ca. 40% within Khotang district, so comparison could be carried out against a weighted averaged of the two. The observed wheat production so averaged during 2003–2013 was $E[Y_w]_{obs} = 1.59$ tonha^{-1}, with coefficient of variation $CV[Y_w]_{obs} = 0.23$. Modeled values where $E[Y_w]_{mod} = 1.45$ tonha^{-1}, with $CV[Y_w]_{mod} = 0.28$. For rice we had $E[Y_r]_{obs} = 2.08$ tonha^{-1}, $CV[Y_r]_{obs} = 0.08$, and $E[Y_r]_{mod} = 2.19$ tonha^{-1}, $CV[Y_r]_{mod} = 0.32$, and for maize $E[Y_m]_{obs} = 2.13$ tonha^{-1}, $CV[Y_m]_{obs} = 0.15$, and $E[Y_m]_{mod} = 2.16$ tonha^{-1}, $CV[Y_m]_{mod} = 0.38$.

Concerning wheat, *Poly-Crop* provides slightly lower yield (−9%) than the observed one, however with well reproduced variability. Rice (+5%), and especially maize (+1%), are better reproduced. For the latter two however variability from *Poly-Crop* simulation is larger than from observations.

5.2. Future climate scenarios

In Table 6, the main future climate scenarios are presented. Therein,

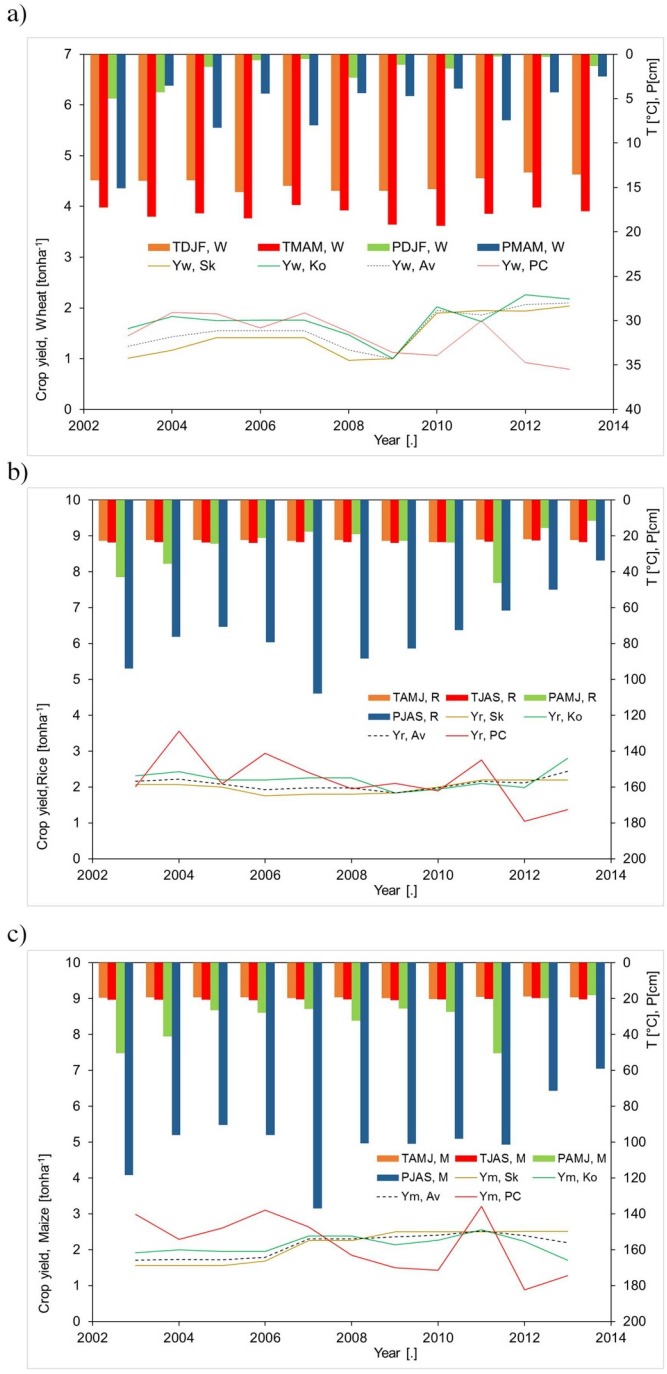

Fig. 2. Dudh Koshi catchment. *Poly-Crop* simulated yield against values from Ministry of Agriculture (2013a). Sk is Solukhumbu, Ko is Kotang, Av is weighted average, PC is modeled by *Poly-Crop*. Average temperature *T*, and precipitation *P* during growth season also reported, split in trimesters (wheat, NDJ, FMA, rice/maize AMJ, JAS). Different values in the same periods mirror differences in altitude range of crops. (a) Wheat. (b) Rice. (c) Maize.

we report the CO_2 atmospheric concentration adopted within the GCM models, the values of *T*, and *P* averaged on the catchment during the growth season (wheat, DNJ, FMA, rice/maize, AMJ, JAS), as projected by the three models under the three RCPs used here after downscaling, against the CR period.

5.3. Future land occupation for cropping

Fig. 3 reports the historical (1975–2010) evolution of population, per capita per day requirement C_n, nutritional power available C_a, and nutritional index $C_{\%}$. With hollow indicators we also report projected values. Visibly, the population increase ever since the '70s carried a corresponding increase of caloric demand C_n, and subsequently of available caloric power C_a. Nutritional index $C_{\%}$, roughly indicating the capability of the cropping system to fulfill nutritional demand in the Dudh Koshi area, increased subsequently, from ca. 71% in 1975, to ca. 111% in 2010 (with a slight decrease to 65% in 1990). Notice that present population projections for Nepal (and the Dudh Koshi area) carry at 2100 a visible decrease, so making nutritional requirements lower than at mid-century, and driving a visible decrease of cropping areas in our simplistic model.

Fig. 4 provides historical land occupation in altitude (500 m altitude belts) for the three target cereals, and projected (2050, 2100) values according to simplified linear regression. From Fig. 4c, maize cropping seems deemed to increase largely, especially at the highest altitudes, 1500–2500 m a.s.l. In Fig. 4a wheat seems to be expectedly increasing its area between 500 and 1500 m a.s.l., as clearly seen historically for increasing population (with a peak in 1990, and substantial stability thereafter). Rice in Fig. 4b seemingly displays an opposite trend. Under population growth historically, the cropping area for rice seemingly decreased at the intermediate altitudes (250–1500 m a.s.l.), with some increase above there (1500–1800 m a.s.l.), and accordingly future projections tend to increase cropped areas in that belt.

5.4. Future crop yield scenarios, and food security

Average values of crop yield for each decade, GCM model, and RCP are reported in Table 7, for both the case of unchanged cropping areas (i.e. with cropped areas equal to the last observed values of 2010), and modified cropped area (indicated with ML, modified land use, as reported in Fig. 4 above). Fig. 6 reports present, and projected (2050, 2100) altitudinal distribution of cropland, and projected crop yield as a function of altitude. Fig. 7 report the corresponding projected values of the nutritional index $C_{\%}$ against present CR value (2010), in both cases of constant, and modified land use (ML). Here we assumed $C_n = 1940–2544$ $\text{Cald}^{-1}\text{p}^{-1}$ as per 2010 values, as provided in the literature.

5.5. Correlation analysis

In Table 8, we report the results of correlation analysis. For Wheat, significant positive correlation ($\rho = 0.55$) is observed against *P* during spring (FMA), and, albeit smaller ($\rho = -0.28$) negative correlation against *T* during the same period. CO_2 seems not visibly impacting wheat yield. As an interesting exception, wheat yield displays a slight, and yet significant positive dependence against T_{NDJ} ($\rho = 0.20$), i.e. increasing temperature during fall-winter may provide a benefit to wheat yield.

Rice displays significant positive correlation ($\rho = 0.79$) with spring (AMJ) *P*, and negative correlation with spring (AMJ) *T* ($\rho = -0.44$). Again here, CO_2 seems not visibly impacting rice production. Maize similarly displays positive correlation ($\rho = 0.53$) with spring P_{AMJ}, and negative correlation with T_{AMJ} ($\rho = -0.55$). Here CO_2 seems slightly (anti)-correlated to maize yield ($\rho = -0.21$).

6. Discussion

6.1. Crop modeling accuracy

The *Poly-Crop* model could be set up and tuned to mimic reasonably well yield of our three crops. $RMSE_{\%}$ is calculated into $RMSE_{\%} = 34\%$, 34%, and 48% for wheat, rice, and maize respectively, somewhat higher than normally accepted for accurate crop modeling (ca. 20% or so, e.g. Cho et al., 2007; Nana et al., 2014). Also as reported, simulated interannual crop yield variability was slightly higher than its observed

Table 5
Dudh Koshi catchment. *Poly-Crop* model validation (2003–2013). Crop yield reported, wheat Y_w, rice Y_r, maize Y_m. Observed values Y_{obs} given for district Solukhumbu, Kotang, and weighed average. Modeled values Y_{mod} provided. Mean and coefficient of variation reported for reference. Random Mean Square Error $RSME_{\%}$ calculated against weighted yield.

District/model	Solukhumbu			Kotang			Weighted			*Poly-Crop*		
	Y_w	Y_r	Y_m	Y_w	Y_r	Y_m	Y_w	Y_r	Y_m	Y_w	Y_r	Y_m
Year	tonha^{-1}	tonha^{-1}	tonha^{-1}	tonha^{-1}	tonha^{-1}	tonha^{-1}	tonha^{-1}	tonha^{-1}	tonha^{-1}	tonha^{-1}	tonha^{-1}	tonha^{-1}
2003	1.01	2.07	1.56	1.59	2.31	1.92	1.24	2.17	1.70	1.45	2.01	2.99
2004	1.17	2.07	1.56	1.83	2.43	2	1.43	2.21	1.74	1.91	3.56	2.29
2005	1.41	2	1.56	1.75	2.2	1.95	1.55	2.08	1.72	1.88	2.09	2.60
2006	1.41	1.75	1.68	1.76	2.2	1.95	1.55	1.93	1.79	1.61	2.94	3.10
2007	1.41	1.8	2.25	1.76	2.25	2.38	1.55	1.98	2.30	1.90	2.40	2.64
2008	0.97	1.8	2.25	1.47	2.25	2.38	1.17	1.98	2.30	1.53	1.95	1.84
2009	1	1.84	2.5	1	1.84	2.14	1.00	1.84	2.36	1.12	2.11	1.50
2010	1.9	2	2.5	2.02	1.94	2.26	1.95	1.98	2.40	1.07	1.90	1.42
2011	1.95	2.2	2.5	1.73	2.1	2.56	1.86	2.16	2.52	1.74	2.76	3.21
2012	1.94	2.2	2.51	2.26	1.99	2.23	2.07	2.12	2.40	0.93	1.04	0.88
2013	2.04	2.2	2.51	2.18	2.8	1.71	2.10	2.44	2.19	0.79	1.37	1.27
E[*Y*]	1.47	1.99	2.13	1.76	2.21	2.13	1.59	2.08	2.13	1.45	2.19	2.16
CV[*Y*] [.]	0.28	0.09	0.21	0.20	0.12	0.12	0.23	0.08	0.15	0.28	0.32	0.38
$RMSE_{\%}$[%]	–	–	–	–	–	–	–	–	–	34	34	48

counterpart. Such circumstance may however depend on the fact that *Poly-Crop* is a spatially distributed model, while normally point-wise assessment is pursued, and it is basically driven by weather, and slight variations of such input may change visibly crop yield. For instance, in 2011 Y_m peaks after a large precipitation spell. During 2012 instead, low precipitation decreased Y_r and Y_m (MOAD, 2013b). Rice yield has a peak in 2004, when precipitation during the year was evenly distributed (not shown). In some years under the occurrence of meteorological variability, the sowing date might have been slightly changed by farmers, or similar adaptation measures might have been applied, that might have smoothed yield variability. *Poly-Crop* performance seems accordingly acceptable, also given the large altitudinal excursion here, and the lack of local accurate information of crop practices and adaptation, and yield.

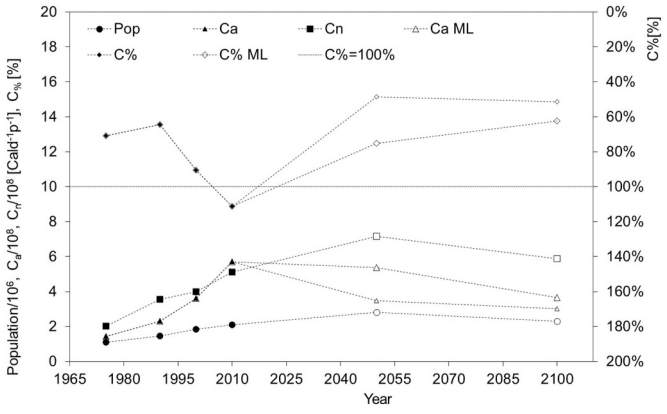

Fig. 3. Dudh Koshi catchment. Population, per capita per day requirement C_n, nutritional power available C_a, and nutritional index $C_{\%}$ (values upside down, right y axis). Hollow indicators provide projected values. ML indicates projections with modified land use at 2050, 2100.

6.2. Climate scenarios

Substantially all GCMs depict a warming weather during the growth season until half century, and further at the end of century (Table 6).

Table 6
Dudh Koshi catchment. Basin averaged decadal projected values of *T*, *P* during growth seasons of crops (split in two trimesters as explained in text), and CO_2 concentration according to the chosen RCPs. CR values also reported, during 2003–2013.

			Y_w	Y_w	Y_r/Y_m	Y_r/Y_m	Y_w	Y_w	Y_r/Y_m	Y_r/Y_m	$Y_w/Y_r/Y_m$
Period	RCP/CR	GCM/obs	TNDJ	TFMA	TAMJ	TJAS	PNDJ	PFMA	PAMJ	PJAS	CO_2
2003–2013	**CR**	**Obs**	3.6	5.8	10.7	12.9	10.1	33.5	101.5	314.6	350
2040–2050	**RCP 2.6**	**EC-Earth**	3.9	6.4	11.4	13.5	4.8	35.4	85.1	322.9	441
		CCSM4	4.2	5.9	11.3	13.5	12.4	61.6	102.2	356.1	441
		ECHAM6	4.1	5.9	10.9	13.3	20.3	28.4	124.1	315.5	441
	RCP 4.5	**EC-Earth**	4.4	6.9	12.0	13.8	4.3	32.1	94.5	351.3	474
		CCSM4	4.7	6.4	11.7	13.6	15.8	43.4	84.4	341.4	474
		ECHAM6	4.3	6.2	11.4	13.8	15.5	28.2	114.4	325.4	474
	RCP 8.5	**EC-Earth**	4.5	7.0	12.1	14.2	6.7	50.2	104.5	337.5	515
		CCSM4	5.1	6.9	11.9	14.2	16.7	49.7	80.6	334.4	515
		ECHAM6	4.8	7.1	12.8	14.5	13.6	19.8	84.9	305.2	515
2090–2100	**RCP 2.6**	**EC-Earth**	4.1	6.4	11.2	13.3	12.5	54.5	94.9	305.9	423
		CCSM4	4.1	6.4	11.4	13.4	11.3	48.2	81.2	328.6	423
		ECHAM6	3.6	5.9	10.7	13.2	17.6	39.1	110.1	332.6	423
	RCP 4.5	**EC-Earth**	5.2	7.7	12.5	14.5	10.7	37.1	95.7	328.9	536
		CCSM4	5.2	7.5	12.5	14.3	14.9	41.6	61.0	365.2	536
		ECHAM6	5.4	8.0	12.5	14.6	17.9	20.2	115.4	289.4	536
	RCP 8.5	**EC-Earth**	7.3	10.4	15.0	16.6	5.9	45.4	111.0	357.0	890
		CCSM4	7.6	9.9	14.7	16.1	19.1	48.7	89.0	376.3	890
		ECHAM6	8.0	9.7	15.5	16.8	15.7	26.3	92.9	352.0	890

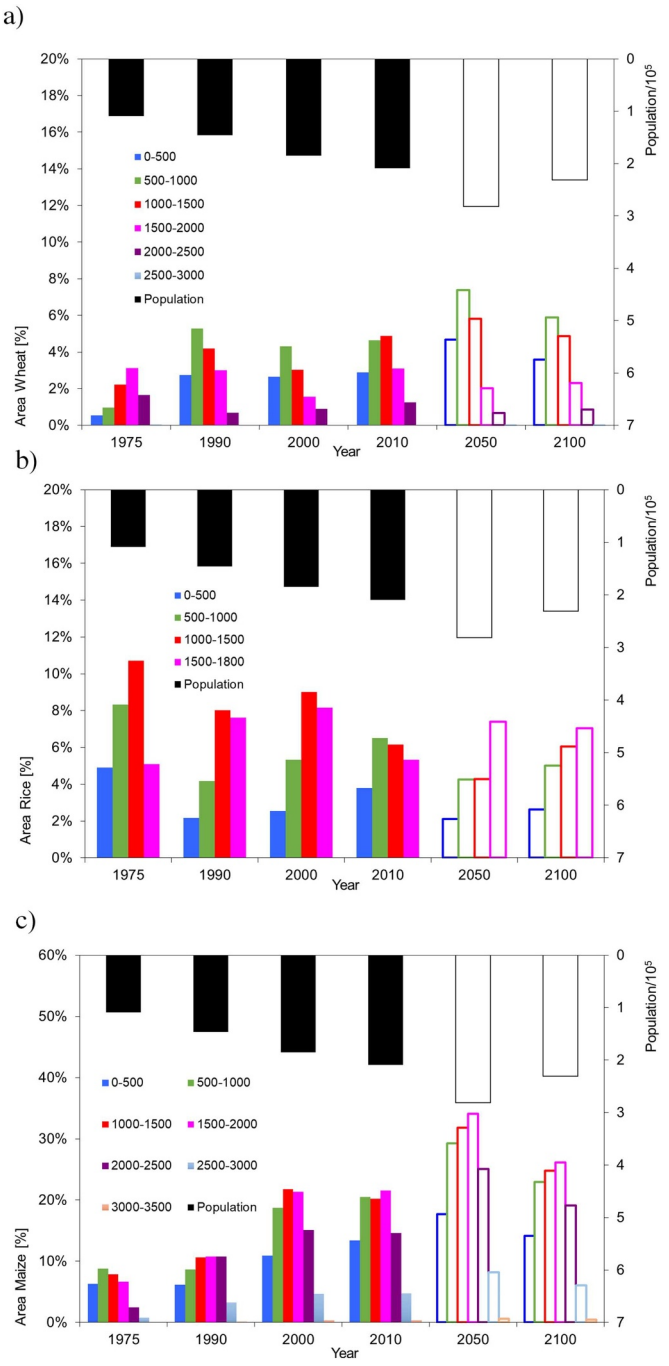

Fig. 4. Dudh Koshi catchment. Historical, and projected land cover for cropping against population (population values upside down, right y axis). Percentage given against available area in the altitude belt. Hollow bars indicate projected values. (a) Wheat. (b) Rice. (c) Maize.

The most sensitive period for wheat according to our analysis is winter-spring trimester (here FMA), when temperature T_{FMA} (anti-correlated with yield) is projected to increase by +0.1 °C (CCSM4, CCSM4, ECHAM6 under RCP 2.6) to +1.3 °C (ECHAM6 under RCP 8.5) until 2050, and by +0.1 °C (ECHAM6 under RCP 2.6) to +4.6 °C (EC-Earth under RCP 8.5), with somewhat large variability.

Rice, and maize display largest anti-correlation against temperature in spring T_{AMJ}, which rises by +0.2 °C (ECHAM6 under RCP 2.6) to +2.1 °C (ECHAM6 under RCP 8.5) until 2050, and by +0 °C (i.e. equal to CR, ECHAM6 under RCP 2.6) to +4.8 °C (ECHAM6 under RCP 8.5), again largely variable.

Table 7
Dudh Koshi catchment. Basin averaged decadal projected values of *Crop yield Y*, for wheat Y_w, rice Y_r, maize Y_m, with present and modified land use ML. CR values also reported, during 2003–2013.

Period	RCP/CR	GCM/Obs	Y_w	Y_wML	Y_r	Y_rML	Y_m	Y_mML
2003–2013	CR	Obs	1.45	1.45	2.19	2.19	2.16	2.16
2040–2050	**RCP 2.6**	**EC-Earth**	1.26	0.88	1.63	1.87	1.22	1.26
		CCSM4	1.19	0.84	1.63	1.78	1.43	1.46
		ECHAM6	1.26	0.89	0.89	1.93	1.61	1.65
		Mean (3 models)	1.24	0.87	1.38	1.86	1.42	1.46
	RCP 4.5	**EC-Earth**	1.21	0.84	1.74	1.86	1.35	1.39
		CCSM4	1.23	0.88	1.27	1.83	1.46	1.49
		ECHAM6	1.18	0.83	1.02	1.93	1.25	1.27
		Mean (3 models)	1.21	0.85	1.34	1.87	1.35	1.38
	RCP 8.5	**EC-Earth**	1.47	1.03	1.68	1.85	1.77	1.82
		CCSM4	0.72	0.54	1.05	1.82	0.57	0.59
		ECHAM6	1.32	0.94	1.07	1.88	1.41	1.44
		Mean (3 models)	1.17	0.84	1.27	1.85	1.25	1.28
2090–2100	**RCP 2.6**	**EC-Earth**	1.48	1.26	1.62	1.73	1.54	1.54
		CCSM4	1.58	1.34	1.6	1.73	2.01	1.99
		ECHAM6	1.07	0.81	0.75	1.6	1.02	1.05
		Mean (3 models)	1.38	1.14	1.32	1.69	1.52	1.53
	RCP 4.5	**EC-Earth**	1.13	0.94	1.57	1.62	1.36	1.39
		CCSM4	1.02	0.85	1.5	2.16	1.13	1.23
		ECHAM6	0.99	0.82	0.7	1.25	0.78	0.83
		Mean (3 models)	1.05	0.87	1.26	1.68	1.09	1.15
	RCP 8.5	**EC-Earth**	0.89	0.69	1.74	1.85	1.2	1.22
		CCSM4	0.63	0.53	1.06	1.82	0.55	0.55
		ECHAM6	1.02	0.82	0.99	1.68	0.89	0.92
		Mean (3 models)	0.85	0.68	1.26	1.78	0.88	0.90

The direction (±) of precipitation change is variable. P_{FMA}, of interest for wheat yield would change at mid-century by −41% (ECHAM6 under RCP 8.5) to +84% (CCSM4 under RCP 2.6), +16% on average (all GCM/RCP). At 2100 the relative change would be between −40% (ECHAM6 under RCP 4.5) and + 63% (EC-Earth under RCP 2.6), on average + 20%. Precipitation amount during this season is relatively low (CR = 33.5 mm), so even large percentage changes imply low precipitation amount (here, from 19.8 to 61.6 mm).

P_{AMJ} in spring is instead of interest for rice, and maize yield. Changes in P_{AMJ} at mid-century would range between −21% (CCSM4 under RCP 8.5) to +22% (ECHAM6 under RCP 2.6), on average − 4%, with end of century values ranging between −40% (CCSM4 RCP 4.5) to +14% (ECHAM6 under RCP 4.5), on average − 7%. Here absolute values would be between 61.0 and 124.1 mm (CR = 101.5).

Benchmarking of recent studies focusing upon future climate of Nepal (Karmacharya et al., 2007; Palazzoli et al., 2015) indicated substantially similar patterns, with consistently increasing temperature in all seasons, and under all models, and precipitation expected to increase during winter (i.e. up to 10% or more within the end of the century), while during spring a slight decrease (down to −7% or less) would be seen. Accordingly, wheat would profit of increasing precipitation during winter, while during spring decreasing precipitation would hamper other crops' yield. Given that all our cereals' yield (lumped at basin's scale) are adversely affected by changes in temperature (Table 8), it is likely that increase of such variable would provide a decrease in productivity in the area.

6.3. *Wheat yield scenarios*

Wheat grows approximately from November to May. During 2040–2050 wheat would display slight changes (Table 7), most notably for RCP2.6 and RCP4.5, however with a large interannual variability

Table 8
Dudh Koshi catchment. Correlation analysis of basing-averaged crop yield against climate descriptors, temperature *T* and precipitation *P* split in trimesters (wheat, NDJ, FMA, rice/maize AMJ, JAS), and CO_2. In **bold**, significant values ($\alpha = 5\%$).

Crop	TNDJ	TFMA	TAMJ	TJAS	PNDJ	PFMA	PAMJ	PJAS	CO_2
Wheat	**0.20**	**−0.28**	–	–	0.00	**0.55**	–	–	−0.12
Rice	–	–	**−0.44**	**−0.19**	–	–	**0.79**	−0.06	−0.10
Maize	–	–	**−0.55**	**−0.21**	–	–	**0.53**	−0.04	**−0.21**

(standard deviation 0.47–0.79 tonha^{-1}, 0.61 tonha^{-1} on average, not shown), a mark of instability, or food insecurity. Under RCP2.5, and RCP4.5 the three models substantially agree, with yield changes (ref. value 1.45 tonha^{-1}) between −13 to −19% (and − 39%, −41% with ML scenario). RCP8.5 displays contrasting results. ECEarth projects and increase of +1.5% (but −28% with ML), with ECHAM6 yielding −50% (and − 62% with ML). Such difference is very likely given by large differences in precipitation during the winter-spring season (Table 6), most influencing wheat yield (Table 8).

Wheat is a *C3* crop, positively affected by increase of CO_2, so increased yield as from ECEarth may be also given by increased CO_2 concentration under RCP8.5 (515 ppm at 2050).

The decade 2090–2100 (Fig. 7a) displays larger variations with respect to half century, with slightly smaller variability (standard deviation 0.32–0.79 tonha^{-1}, but 0.51 tonha^{-1} on average, not shown). Under RCP2.6, model CCSM4 depicts yield decrease (−26%, −35% ML), but the two other models depict increase (but slight decrease for ML). CCSM4 likely suffers from less P_{NDJ}, and highest T_{NDJ} (+0.7 °C), decreasing yield, especially in the altitude range 2000–2800 m a.s.l. (Fig. 5a). ECHAM6 increases yield by +9%, due to a slight increase of mean temperature (+0.1 °C) T_{NDJ}. ECEarth displays (Table 6) both increasing T_{NDJ} and T_{FMA}, with further increasing P_{FMA}, likely leading to very slightly increased yield. Under RCP4.5 however all models carry decreasing yield between −32% (ECEarth, −35% with ML) and −22% (CCSM4, −43% ML), with differences given by different increase in T_{FMA}. Under RCP8.5, all models depict large loss of yield, and ECHAM6 projects the largest decrease of wheat yield (−57%, −64% ML), likely caused by little precipitation P_{FMA}, and large increase of T_{FMA}. Eventually on average one would have at 2050–16% (−41% ML) yield, and at 2100–25% (−38% ML) yield.

6.4. Rice yield scenarios

During 2040–2050 rice yield would always decrease (Table 7), and changes (against reference value 2.2 tonha^{-1}) range between −21% e −59% (−11.6% to −18.8% with ML). Standard deviation here ranges between 0.24 and 1.10 tonha^{-1}, with 0.64 tonha^{-1} on average. Under scenario RCP 2.6, ECEarth and ECHAM6 display −25% yield (−17% on average with ML), with ECHAM6 displaying however a large interannual variability, with yield reaching up to 2.8 tonha^{-1} in some years, and then reaching very low values of 0.2 tonha^{-1} or so (not shown). Particularly poor harvest is found in year with P_{AMJ} below average (see Table 8 for correlation analysis). RCP 4.5 displays changes in yield between −21% (ECEarth) and − 53% (CCSM4), improved with ML (ca. -16%). The latter model displays low P_{AMJ} (Table 6), and increasing temperature T_{AMJ} (+1 °C vs CR). RCP8.5 gives yield from −23% (ECEarth) to −52% of ECHAM6. On average at 2050 rice yield would reach −39% (and −15% with ML). The decade 2090–2100 has even larger decrease of productivity. Yield decreases by −21% (ECEarth, RCP8.5), to −68% (CCSM4, RCP4.5), again improving with ML (−1% to −43%). Average loss of rice at 2100 would be −42% (and −22% with ML). Standard deviation ranges between 0.18 and 1.10 tonha^{-1}, with 0.57 tonha^{-1} on average.

6.5. Maize yield scenarios

Maize is here the most widespread crop, and possibly the most impacting upon local food security. At 2050 decrease (vs reference value 2.16 tonha^{-1}) is always projected (−73% with ECHAM6 under RCP8.5 to −18% with ECEarth, RCP8.5, average −38%, very slightly improving under ML scenario. Table 7), with large variability (standard deviation ranges between 0.56 and 1.89 tonha^{-1}, with 1.11 tonha^{-1} on average). Generally low yield follows low P_{AMJ} (Fig. 2c). RCP8.5 displays somewhat discordant results, with changes between −18% to −73% as reported. The lowest value comes from ECHAM6 model, which under RCP8.5 displays high T_{AMJ} (+2.1 °C vs CR, Table 6), and low P_{AMJ} (−16% vs CR, Table 6). At 2100 one has always decreased yield (−74% with ECHAM6 under RCP8.5 to −7% with ECHAM6, RCP2.6, average −46%, Table 7), and large variability, albeit smaller than at 2050 (standard deviation between 0.56 and 1.33 tonha^{-1}, with 0.88 tonha^{-1} on average).

6.6. Altitudinal distribution of crop yield

Projected crop yield as a function of altitude in Fig. 5 provide some hints for discussion. According to our results wheat yield (Fig. 5a) is very largely changing with altitude, and reaches a maximum nearby 2800 m a.s.l. or so, thereby rapidly decreasing until 3500 m a.s.l. Therein, very little area is cropped presently, and less would be cropped in the future. Notice that basin area (red dashed line Fig. 5a) has a (relative) maximum nearby 2500 m a.s.l. or so, which would suggest some chance for expansion.

At 2100, decrease of yield would continue at the lowest altitudes, so requiring further uplifting. Under RCP8.5, leading to considerable temperature increase as reported, optimal (i.e. comparable to now) crop yield would be lifted up to 3600 m a.s.l. or more. Thus, at the end of century large uplifting of wheat would be required, whenever possible given land availability, and winter climate. This is contrary to the present trend, displaying decrease (or stability) of wheat areas in the highest altitudes.

Rice (Fig. 5b) displays increasing yield against altitude, up to 1800 m a.s.l., where indeed rice cropping ends. Rice area distribution basically follows the yield potential up to 1600 m a.s.l. or so, with a subsequent decrease. ML scenario here indicates a potential for future expansion upward, so aiding adaptation to climate change by increasing mean yield.

At 2050, rice yield is lower than CR at all simulated altitudes, and similarly until 2100, with the sole exception of ECEarth under RCP8.5. Given that no rice is harvested insofar at higher altitudes than shown here, we pursued no simulation of rice productivity above there. However, it is possible that at higher altitudes rice may provide larger yield.

Maize, largely the most harvested cereal here, has a more complex response in altitude. It displays a large plateau of highest productivity between 2000 and 3000 m a.s.l., likely a good reason for large use of this crop in Dudh Koshi basin. However, most of crop area for maize is at lower altitude (peak at 1500 m a.s.l. or so), which would indicate that maize cropping may need moving to higher altitudes than now, where also large area is available.

At midcentury, productivity would decrease largely under RCP8.5,

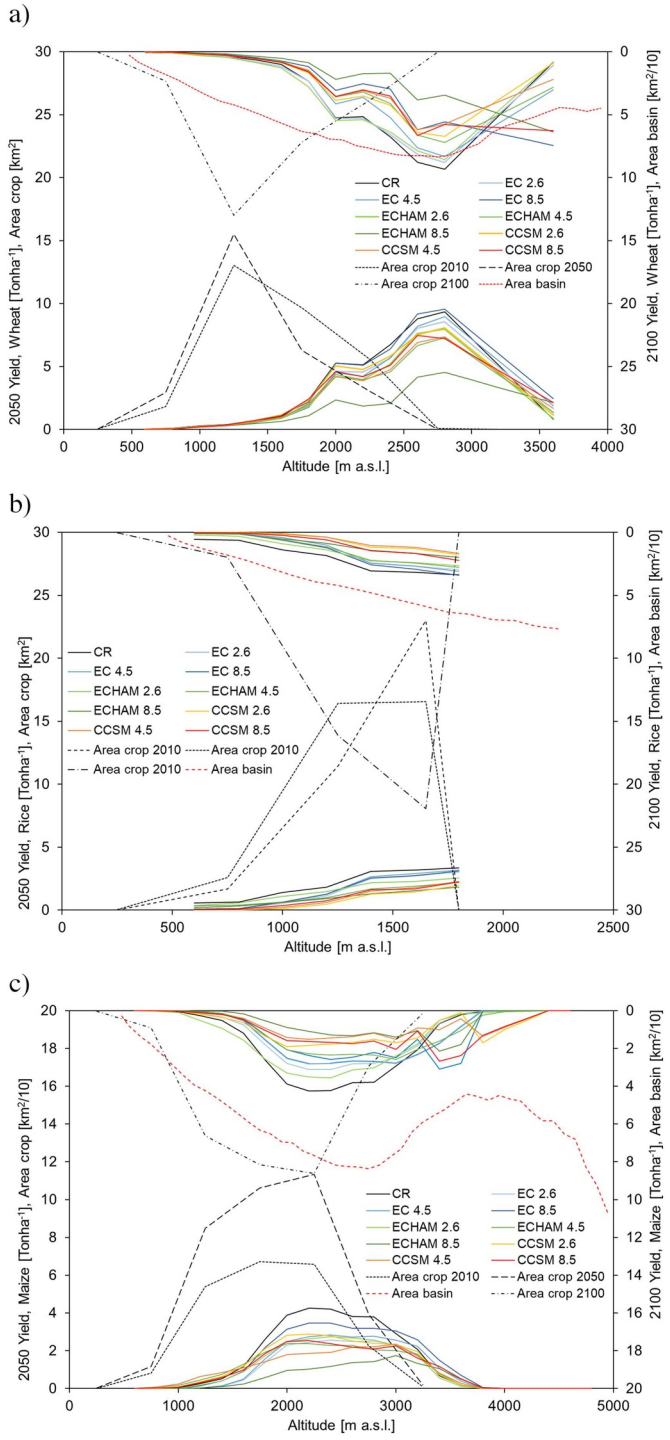

Fig. 5. Dudh Koshi catchment. *Poly-Crop* simulated yield as per altitude belts, GCMs, and RCPs, 2050, and 2100 (right y axis, values upside-down). Present (2010), and projected (2050, 2100) altitudinal distribution of crop areas for each crop (in km^2, or km^2/10 for readability) is reported, together with altitudinal distribution of basin's area (hypsography, in km^2, or km^2/10 for readability) within the altitude range of the crop. (a) Wheat. (b) Rice. (c) Maize.

with however some gain above 3000 m a.s.l. or so. At 2100 productivity curve would be in practice flat, with largely increased productivity until 3600 m a.s.l. or so, given temperature increase in this area. Consistently, the ML scenario displays a trend to occupy larger areas at the highest altitudes for maize cropping.

As a benchmark, Bhatt et al. (2014) assessed crop yield (1967–2008) against climate for wheat, rice and maize within the

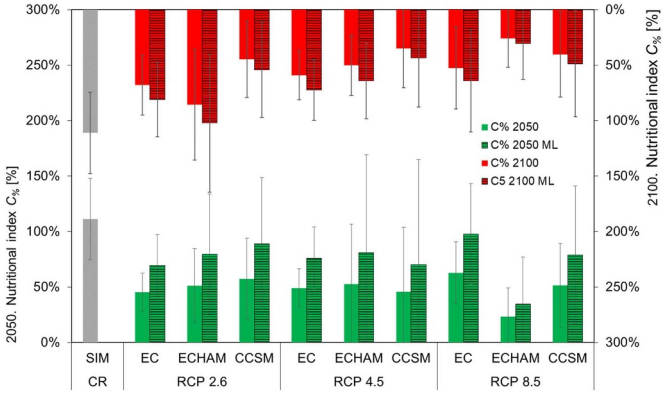

Fig. 6. Dudh Koshi catchment. Nutritional index $C_{\%}$, present (2010), and projected (2050, 2100, the latter upside down, right vertical axis). ML indicates projections with modified land use at 2050, 2100. Decadal average, and confidence limits (± 1 standard deviation) given.

(Sapt) Koshi river, as per different altitude belts. They assessed trends of T_g and P_g and successively highlighted the influence of such trends upon yield Y by way of multiple regression, applied to each crop in each district with available data. For Y_w, they found negative effects of high temperatures, especially at low altitudes (1200–1700 m a.s.l.) during NDJF, consistently with our findings here (Fig. 6a, displaying very low yield within that altitude belt). For Y_r, they highlighted a negative correlation against T_g especially during the first phase (spring), mostly pronounced between 1300 and 1700 m a.s.l., again consistent with our findings of negative response of rice yield to high temperature in spring (Tables 6, 7, 8).

For Y_m, positive correlation against T_g was found during March, and April, and negative during July and August (after flowering), mostly visible between 1200 and 1650 m a.s.l. Here we found negative correlation of Y_m vs T_{AMJ}, and less vs T_{JAS} (Fig. 2c, Table 8), and however relatively low yield at such low altitudes (Fig. 5c). Bhatt et al. (2014) found P_g to be positively correlated with Y_w, and Y_m, and negatively (weakly) with Y_r. However, no distinction was made between irrigated and rain-fed crops, so possibly the effect of precipitation might have been masked.

Analysis of climate trends in Bhatt et al. (2014) displayed in most cases a decrease of Y against T_g. In some high altitude areas however, rice and maize displayed positive feedback against increasing temperatures. Here in Fig. 5b,c such crops already have largest productivity at the highest edge of their range (especially rice), and future increase of temperature under climate change may further favor yield higher up (especially for maize).

6.7. Cropland expansion and food security

Our approach indicated in practice an increase of cropping altitude to comply with nutritional requirement, at least for the case of rice, and maize, with wheat displaying a somewhat less clear signal. Our projected trends of land occupation thus indicate potential for improved fulfilment of nutritional demand, and food security by occupation of the highest altitudes. Clearly such occupation increases available yield by a two-fold mechanism, namely by (i) increase of cropped area, and (ii) adaptation to potential climate change with (at least partial) recovery of yield.

Fig. 6 clearly indicates a potential (in some cases very large, down to 23% vs 110% now) decrease of the nutritional index under future climate change, if no change in land use would be pursued This could be made up for (in some cases largely) by cropping at higher altitudes than now.

According to our analysis, during 1975–2010 the contribution of maize C_a ranged between 56 and 89%, ever increasing, with Rice

making 27–4%, and wheat 17–7%, ever decreasing, mostly given by the much larger occupied area for maize. At 2050, in response to even larger occupation for maize cropping as projected, maize would occupy 84% (and 91% under ML) of C_a on average, with Rice at 10% (and 5% under ML), and Wheat at 6% (the same under ML), given by somewhat better resilience of rice to climate change, but large occupation of land for maize cropping under the ML scenario. At 2100 the share would be 84%, 6%, and 10%, respectively (and 89%, 5%, and 6% under ML). Under our projections therefore maize would remain a largely contributing crop, especially whenever large expansion of this cereal would occur. From Fig. 6, large variability of $C_{\%}$ is observed (as from standard deviation of the decadal yield). Under ML scenario $C_{\%}$ variability is even higher than under unchanged land use, especially at 2050, because of the larger share carried by maize on $C_{\%}$, decreasing largely the nutritional index for years with low maize yield.

6.8. Limitations and outlooks

The *Poly-Crop* model we used here makes a number of simplifying assumptions with respect to other softwares (e.g CropSyst, Confalonieri et al., 2009, SWAT, Schuol et al., 2008), including use of one single soil layer, and depiction of soil properties, and of crop phenology using fewer parameters (Table 3). Full availability of nutrients is hypothesized, which is not granted, albeit likely not relevant in our target area here. With such caveats, our *Poly-Crop* model seems to perform well in depicting growth of our three cereals. Some uncertainty may dwell into land use classification for cropping, which cascades into assessment of mean yield at basin scale. As reported, we had to slightly modify ICIMOD maps (Kabir et al., 2015) for crop cover, however with results that are consistent with Nepal statistics of land cover, and with maximum growth of each crop as from satellite data.

Poly-Crop model accounts for CO_2 changes using the method by Stöckle et al. (1992), supposedly valid for 330–660 ppm. It is not clear known what would happen for higher concentration of CO_2, like those projected under RCP8.5 at 2100. Some studies (free air CO_2 experiments FACE, e.g. Kim et al., 2003; McMurtrie et al., 2008) demonstrated that for CO_2 concentration as high as 700 ppm biomass growth of *C3* plants may change (i.e. be either amplified o r reduced) under water, and nutrient limitation. The results here for very large CO_2 concentration may be critical, and one has to verify the response of crops under such conditions.

Future outlooks in Dudh Koshi region include assessment of potential adaptation strategies for future climate change, use of irrigation to make up for water stress (e.g. Bocchiola et al., 2013; Bocchiola, 2015), anticipation of sowing date, and possibly use of modified (i.e. slower maturing) cultivars (i.e. with higher heat units, e.g. Tubiello et al., 2000; Torriani et al., 2007), also varying with altitude, given the complex structure of vertical response of crops to climate as reported. Land use changes in the future, also limited by a complex set of drivers need be explored, to assess potential for adaptation.

L arge uncertainty is brought about by different o utcomes from GCMs/RRCPs. Rainfall variability between models, and RCPs plays a large role in modifying crop patterns.

RCP2.6 and RCP8.5 depict in practice more extreme pathways (i.e. either very optimistic, or very pessimistic), with RCP4.5 depicting an intermediate situation. Recent findings (Fuss et al., 2014) indicated that recent temperature evolution overlaps well with the projected pattern of RCP8.5 of IPCC, i.e. warming recently proceeded according to the most pessimistic scenarios. Seemingly if projections need be made now, globally one may expect that the most credible scenarios here are those under RCP8.5.

Clearly, exploitation of land for agricultural purposes, which we depicted here preliminarily as solely driven by population, and thus by need for increased yield, is driven by other processes.

Recent works have explored drivers for changes in cropland status, and agricultural land occupation under climate change in Nepal. Paudel et al. (2016a, 2016b) studied changes in cropland status and its drivers in the (Sapt) Koshi river, between 1978 and 2010. They found rapid increase of croplands since 1978 onward, at differing rates and to different extents. Cropland area covered 7165 km^2 in 1978, peaked 7867 km^2 in 1992, and reduced slightly to 7777 km^2 by 2010. Using logistic regression, they associated changes in cropland area to four potential driving factors, namely topography (elevation, slope, and soil type), socioeconomics (population and foreign labor migration), climate (annual mean temperature and precipitation), and neighborhood factors (roads, rivers, and settlements). Socioeconomic factors had a major role in cropland change, with the increasing population density being ranked in 1st position. Then, elevation, slope, and soil types were important driving factors of cropland change. Especially, they observed high-altitude cropland areas that had been abandoned due to the difficulties of management, and generally altitude was a stronger driver for land abandonment than for occupation. They found that cropland is mostly concentrated within a range of slope of 14–30°, with however little agricultural activities in areas with a slope > 25°, and that large slope was a main driver of cropland contraction. In Dudh Koshi here, preliminary analysis (Polinelli, 2017) indicated that, further to population growth, potential drivers of land use change may include climate (temperature, precipitation), topography (altitude, slope, aspect), and network (distance to road) act as limiting, or conditioning factors. Future work will attempt at including such variables in our analysis.

Our nutritional index here simply considered a mix of the three studied crops. Clearly, diet complexity in Nepal, as in any other country, makes such simple assumption unfit to fully describe fulfilment of dietary needs, and food security. However, we found that crop area/yield actually followed historical population development in the target area, and caloric needs therein, so our simplified approach seems indicative, at least in term of relative variation of available energy power as given by the studied crops, and food security therein.

The results in Fig. 6 indicate clearly that cropland expansion may partially make up for decreased yield under climate change. However, large dependence on maize yield as per large land occupation recently (and projected) may result into larger variability. Accordingly, a more balanced mix of crops needs to be attained, and may be explored further on.

7. Conclusions

Our “what if” study provides insights of the potential fallout of global warming upon *food security* of the population living in the Dudh Koshi catchment of Nepal, a country heavily sensitive to climate change. Notwithstanding the relatively sparse knowledge of crop productivity in this area, and of its variability with topography and climate, the *Poly-Crop* model could be used to provide a representative depiction of distributed crop yield within the catchment.

In spite of some uncertainty in absolute values, the results here provided are consistent between different models, and RCPs, in terms of prospective impacts on crops. With constant agricultural land use, on average wheat yield would decrease at 2100, with largely increased yearly variability. Seemingly lifting of wheat cropland to highest altitudes may be useful to maintain present yield, especially in rain fed conditions as here, with irrigation being necessary during winter-spring FMA. However, historical trends as observed in the area, would lead to project decreased wheat area along the century, with even larger decrease of wheat yield.

Rice yield would be lower on average at midcentury, and at 2100 (−42%), with interannual variability slightly smaller than now. Seemingly from our results, rice may profit from the projected increasing altitude of croplands, and possibly by irrigation especially during spring AMJ.

Maize would also decrease yield until midcentury, and 2100, with much larger variability than now, and may require irrigation during AMJ given its large water consuming nature. However, increased

altitude of maize cropping would provide slightly improved yield, and much larger nutritional contribution as per increased cropped area. Our results show that climate change may put at stake *food security* in the Dudh Koshi catchment, and in the high altitude areas of Nepal in the near and mid-term future. Food demand in the country is going to increase due to the growing population and consumption patterns, as did in the past, and dependable crop yield is needed. Our work here may contribute to assessment of future food security, and subsequent adaptation under a scientifically driven, quantitative framework.

Acknowledgments

The present work was carried out with support from SHARE-Paprika, and SHARE-Koshi projects, funded by the EVK2CNR Association of Italy, kindly acknowledged. Support and computational power for the development of crop and hydrological modeling was given by Climate-L ab, an interdepartmental laboratory on climate change of Politecnico di Milano. We hereby acknowledge the Department of Hydro Meteorology (DHM) of Nepal, for providing weather data from their stations. Nepal Academy of Science and Technology (NAST) is acknowledged for providing personnel and logistic assistance. Mr. Gianpietro Verza, and Dr. Elisa Vuillermoz, technical coordinators of Pyramid laboratory, and the Pyramid staff are kindly acknowledged for support, and assistance during field campaign and for data delivery. We acknowledge the World Climate Research Programme's Working Group on Coupled Modeling, which is responsible for CMIP, and the climate modeling groups (listed in Table 4 of this paper) for producing and making available their model outputs. For CMIP the Program for Climate Model Diagnosis and Intercomparison PCMDI of the US Department of Energy provides coordinating support and led development of software infrastructure in partnership with the “Global Organization for Earth System Science Portals”. We acknowledge help from two anonymous reviewers, to improve the manuscript for publication.

References

Addimando, N., Nana, E., Bocchiola, D., 2015. Modeling pasture dynamics in a mediterranean environment: Case study in sardinia, Italy. J. Irrig. Drain. Eng. 141 (5) (04014063-1).

Agarwal, A., Babel, M.S., Maskey, S., 2014. Analysis of future precipitation in the Koshi River basin, Nepal. J. Hydrol. https://doi.org/10.1016/j.jhydrol.2014.03.047.

Awasthi, K.D., Sitaula, B.K., Singh, B.R., Bajacharaya, R.M., 2002. Land-use change in two Nepalese watersheds: GIS and geomorphometric analysis. Land Degrad. Dev. 13 (6), 495–513.

Bartlett, R., Freeman, S., Cook, J., Dongol, B.S., Sherchan, R., Shrestha, M., McCornick, P.G., 2011. Freshwater Ecosystem Vulnerability Assessment: The Indrawati Sub-Basin, Nepal, Nicholas Institute for Environmental Policy Solutions Report, NI R 11-07. Duke University, WWF.

Bhatt, D., Maskey, S., Babel, M.S., Uhlenbrook, S., Prasad, K.P., 2014. Climate trends and impacts on crop production in the Koshi River basin of Nepal. Reg. Environ. Chang. 14, 1291. https://doi.org/10.1007/s10113-013-0576-6.

Bhattarai, M., Pant, D., Mishra, V.S., Devkota, H., Pun, S., Kayastha, R.N., Molden, D., 2002. Integrated Development and Management of Water Resources for Productive and Equitable Use in the Indrawati River Basin, Nepal (Working Paper 41). International Water Management Institute (IWMI), Colombo, Sri Lanka.

Bocchiola, D., 2007. Use of scale recursive estimation for multisensor rainfall assimilation: a case study using data from TRMM (PR and TMI) and NEXRAD. Adv. Water Resour. 30, 2354–2372.

Bocchiola, D., 2015. Impact of potential climate change on crop yield and water footprint of rice in the Po Valley of Italy. Agric. Syst. 139, 223–237.

Bocchiola, D., 2017. Agriculture and food security under climate change in Nepal. Adv. Plants Agric. Res. 6 (6), 00237. 2017. 10.15406/apar.2017.06.00237.

Bocchiola, D., Rosso, R., 2006. The use of scale recursive estimation for short term Quantitative Precipitation Forecast. Phys. Chem. Earth 31 (18), 1228–1239.

Bocchiola, D., Soncini, A., 2017. Pasture modelling in mountain areas: the case of Italian Alps, and Pakistani Karakoram. Agric. Res. Technol. 8 (3), 555736.

Bocchiola, D., Nana, E., Soncini, A., 2013. Impact of climate change scenarios on crop yield and water footprint of maize in the Po valley of Italy. Agric. Water Manag. 116, 50–61.

Bookhagen, B., Burbank, D.W., 2010. Toward a complete Himalayan hydrological budget: spatiotemporal distribution of snowmelt and rainfall and their impact on river discharge. J. Geophys. Res. Earth Surf. 115 (F3) 2003 – 2012.

Brouwer, F.M., 1988. Determination of Broad-Scale Land Use Changes by Climate and Soils. Working Paper WP-88-007. International Institute for Applied Systems Analysis, Laxenburg, Austria.

Campbell, G.S., 1985. Soil physics with Basic: transport models for soil–plant systems. Elsevier, Amsterdam 149 pgs. ISBN: 9780080869827.

Cho, M.A., Skidmore, A.C.F., van Wieren, S.E., Sobhan, I., 2007. Estimation of green grass/herb biomass from airborne hyperspectral imagery using spectral indices and partial least squares regression. Int. J. Appl. Earth Obs. Geoinf. 9, 414–424.

Confalonieri, R., Acutis, M. Gianni Bellocchi, G., Donatelli, M., 2009. Multi-metric evaluation of the models WARM, CropSyst and WOFOST for rice. Ecol. Model. 220 (11), 1395–1410.

Cook, S., Rubiano, J., Sullivan, C., Andah, W., Ashante, F., Wallace, J., Terrasson, I., Nikiema, A., Kemp-Benedict, E., Tourino, I., Yiran, G.A.B., 2007. Water poverty mapping in the Volta basin. In: CGIAR Challenge Program on Water and Food, Workshop Report, Accra, Ghana 3–8 March, . http://cpwfbfp.pbworks.com/f/Water_poverty_mapping_Volta_Ghana_Workshop_Report.pdf.

Devkota, L.P., Gyawali, D.R., 2015. Impacts of climate change on hydrological regime and water resources management of the Koshi River Basin. Nepal. J. Hydrol. 4, 502–515 Regional Studies.

Dulal, H.B., Brodnig, G., Thakur, H.K., Green-Onoriose, C., 2010. Do the poor have what they need to adapt to climate change? A case study of Nepal. Local Environ. 15 (7), 621–635.

Eriksson, M., Xu, J.C., Shrestha, A.B., Vaidya, R.A., Santosh, N., Sandström, K., 2009a. The Changing Himalayas: Impact of Climate Change on Water Resources and Livelihoods in the Greater Himalayas. 978-92-9115-111-0.

Eriksson, M., Jianchu, X., Shrestha, A.B., Vaidya, R.A., Nepal, S., Sandström, K., 2009b. Impact of Climate Change on Water Resources and Livelihoods in the Greater Himalayas. ICIMOD, Kathmandu pp.24, ISBN : 9789291151110.

FAO, 2004. The Soil and Terrain database (SOTER) for Nepal. http://www.fao.org/soils-portal/soil-survey/soil-maps-and-databases/regional-and-national-soil-maps-and-databases/en/.

FAO, 2009. Adapting to Climate Change. In Unasylva, 60. (231/232).

FAO, 2016. Food and Nutrition Security in Nepal: A Status Report – Ministry of Agricultural Development and Central Bureau of Statistics for the Nepal component of the FSO Project. http://admin.indiaenvironmentportal.org.in/files/file/Food%20and%20Nutrition%20Security%20in%20Nepal.pdf.

Fuss, S., Canadell, J.G., Peters, G.P., Tavoni, M., Andrew, R.M., Ciais, P., et al., 2014. Betting on negative emissions. Nat. Clim. Chang. 4 (10), 850–853.

Gautam, B.P., Webb, E.L., Shivakoti, G.P., Zoebisc, M.A., 2003. Land use dynamics and landscape change pattern in a mountain watershed in Nepal. Agric. Ecosyst. Environ. 99, 83–96.

Gent, P. R., and twelve co-authors, 2011. The community climate system model version 4. J. Clim. 24, 4973–4991.

Gianinetto, M., Polinelli, F.N., Frassy, F., Aiello, M., Rota Nodari, F., Soncini, A., Bocchiola, D., 2017. Analysis of changes in crop farming in the Dudh Koshi (Nepal) driven by climate changes. In: Conference: Earth Resources and Environmental Remote Sensing/GIS Applications, https://doi.org/10.1117/12.2278637.

Groppelli, B., Bocchiola, D., Rosso, R., 2011a. Spatial downscaling of precipitation from GCMs for climate change projections using random cascades: a case study in Italy. Water Resour. Res. 47, W03519. https://doi.org/10.1029/2010WR009437.

Groppelli, B., Soncini, A., Bocchiola, D., Rosso, R., 2011b. Evaluation of future hydrological cycle under climate change scenarios in a mesoscale Alpine watershed of Italy. NHESS 11, 1769–1785. https://doi.org/10.5194/nhess-11-1769-2011.

Hazeleger, W., and eleven co-authors, 2011. EC-Earth V2.2: description and validation of a new seamless earth system prediction model. Clim. Dyn. J. 39, 2611–2629.

Hengl, T., Mendes de Jesus, J., Heuvelink, G.B.M., Ruiperez Gonzalez, M., Kilibarda, M., et al., 2017. SoilGrids250m: Global Gridded Soil Information Based on Machine Learning. www.soilgrids.org.

Hirano, A., Welch, R., Lang, H., 2003. Mapping from ASTER stereo image data: DEM validation and accuracy assessment. ISPRS J. Photogramm. Remote Sens. 57 (5–6), 356–370.

ICIMOD, 2015. Nepal's Digital Agriculture Atlas. http://geoportal.icimod.org/?q=21298.

ICIMOD, 2017. Regional Data Base Initiative. http://www.icimod.org/?q=rdi.

Immerzeel, W., Petersen, L., Ragettli, S., Pellicciotti, F., 2014. The importance of observed gradients of air temperature and precipitation for modeling runoff from a glacierized watershed in the Nepalese Himalayas. Water Resour. Res. 50 (3), 2212–2226.

IPCC, 2013. Summary for policymakers. In: Stocker, T.F., Qin, D., Plattner, G.-K., Tignor, M., Allen, S.K., Boschung, J., Nauels, A., Xia, Y., Bex, V., Midgley, P.M. (Eds.), Climate Change 2013: The Physical Science Basis. Contribution of Working Group I to the Fifth Assessment Report of the Intergovernmental Panel on Climate Change. Cambridge University Press, Cambridge, United Kingdom and New York, NY, USA.

Jarvis, A.J., Mansfield, T.A., Davies, W.J., 1999. Stomatal behaviour, photosynthesis and transpiration under rising CO_2. Plant Cell Environ. 22, 639–648.

Kabir, U., et al., 2015. Development of 2010 national land cover database for the Nepal. J. Environ. Manag. 148, 82–90. http://rds.icimod.org/.

Karki, R., Gurung, A., 2012. An overview of climate change and its impact on agriculture: a review from least developing country, Nepal. Int. J. Ecosyst. 2 (2), 19–24.

Karmacharya, J., Shrestha, A., Rajbhandari, R., 2007. Climate change scenarios for Nepal based on regional climate Model RegCM3, Department of Hydrology and Meteorology Kathmandu – Nepal. In: Final report of the Project: “Enhancement of National Capacities in the Application of Simulation Models for Assessment of Climate Change and its Impacts on water Resources and Food and Agricultural Production”.

Kim, H.Y., Lieffering, M., Kobayashi, K., Okada, M., Miura, A., 2003. Seasonal changes in the effects of elevated CO_2 on rice at three levels of nitrogen supply: a free air CO_2 enrichment (FACE) experiment. Glob. Chang. Biol. 9 (6), 826–837.

Leuning, R., 1995. A critical appraisal of a combined stomatal photosynthesis model for

C3 plants. Plant Cell Environ. 18, 357–364.
Malla, G., 2008. Climate change and its impact on Nepalese agriculture. J. Agric. Environ. 9, 62–71.
Maskey, S., Uhlenbrook, S., Ojha, S., 2011. An analysis of snow cover changes in the Himalayan region using MODIS snow products and in-situ temperature data. Clim. Chang. 108 (1–2), 391–400.
Matthews, R.B., Pilbeam, C., 2005. Modelling the long-term productivity and soil fertility of maize/millet cropping systems in the mid-hills of Nepal. Agric. Ecosyst. Environ. 111 (1–4), 119–139.
McMurtrie, R.E., Norby, R.J., Medlyn, B.E., Dewar, R.C., Pepper, D.A., Reich, P.B., Barton, C.V.M., 2008. Why is plant-growth response to elevated CO_2 amplified when water is limiting, but reduced when nitrogen is limiting? A growth-optimisation hypothesis. Funct. Plant Biol. 35, 521–534.
MOAD, 2013a. Crop Situation Update. https://sites.google.com/site/nefoodsec/home/crop-situation-update.
MOAD, Ministry of Agricultural Development, Government of Nepal, 2013b. Statistical Information on Nepalese Agriculture, Time Series Information (1999/2000–2011/2012, 2012/2013). http://www.moad.gov.np/uploads/files/TimeSeries_Final_BK.pdf, http://www.moad.gov.np/uploads/files/YearBook%202013.pdf
Monteith, J.L., 1977. Climate and the efficiency of crop production in Britain. Philos. Trans. R. Soc. B281, 277–294.
Morison, J.I.L., 1999. Interactions between increasing CO2 concentration and temperature on plant growth. Plant Cell Environ. 22 (6), 659–682.
Nana, E., Corbari, C., Bocchiola, D., 2014. A hydrologically based model for crop yield and water footprint assessment: study of maize in the Po valley. Agric. Syst. 127, 139–149.
NAPA, 2010. National Adaptation Programme of Action (NAPA). Government of Nepal, Ministry of Environment, Kathmandu, Nepal.
Neupane, N., Ramachandra Murthy, M.S., Rasul, G., Wahid, S., Shrestha, A.B., Uddin, K., 2013. Integrated biophysical and socioeconomic model for adaptation to climate change for agriculture and water in the Koshi Basin. In: Handbook of Climate Change Adaptation, https://doi.org/10.1007/978-3-642-40455-9_77-1.
NGMDA, Nepal Government Ministry Agricultural Development, 2012. Food composition table for Nepal. In: Department of Food Technology and Quality Control. National Nutrition Program, 2012, . http://www.fao.org/fileadmin/templates/food_composition/documents/regional/Nepal_Food_Composition_table_2012.pdf.
Nyaupanea, G.P., Chhetrib, N., 2009. Vulnerability to climate change of nature-based tourism in the Nepalese Himalayas. Tour. Geogr. 11 (1), 95–119.
O'Leary, G.J., Christy, B., Nuttall, J., Huth, N., Cammarano, D., Stöckle, C., Basso, B., Shcherbak, I., Fitzgerald, G., Luo, Q., Farre-Codina, I., Palta, J., Asseng, S., 2015. Response of wheat growth, grain yield and water use to elevated CO2 under a Free-Air CO2 Enrichment (FACE) experiment and modelling in a semi-arid environment. Global Change Biol. 21 (2015), 2670–2686.
Olesen, J.E., Bindi, M., 2002. Consequences of climate change for European agricultural productivity, land use and policy. Eur. J. Agron. 16, 239–262.
Olesen, J.E., Carter, T.R., Diaz-Ambrona, C.H., Fronzek, S., Heidmann, T., Hickler, T., Holt, T., Minguez, M.I., Morales, P., Palutikof, J.P., Quemada, M., Ruiz-Ramos, M., Rubæk, G.H., Sau, F., Smith, B., Sykes, M.T., 2007. Uncertainties in projected impacts of climate change on European agriculture and terrestrial ecosystems based on scenarios from regional climate models. Clim. Chang. 81, 123–143.
Ortiz, R., Sayre, K.D., Govaerts, B., Gupta, R., Subbarao, G.V., Ban, T., Hodson, D., Dixon, J.M., Ortiz-Monasterio, J.I., Reynolds, M., 2008. Climate change: can wheat beat the heat? Agric. Ecosyst. Environ. 126, 46–58.
Palazzoli, I., Maskey, S., Uhlenbrook, S., Nana, E., Bocchiola, D., 2015. Impact of prospective climate change upon water resources and crop yield in the Indrawati basin, Nepal. Agric. Syst. 133, 143–157.
Parry, M.L., Rosenzweig, C., Iglesias, A., Livermore, M., Fischer, G., 2004. Effects of climate change on global food production under SRES emissions and socio-economic scenarios. Glob. Environ. Chang. 14, 53–67.
Paudel, B., Gao, J., Zhang, Y., Wu, X., Li, S., Yan, J., 2016a. Changes in cropland status and their driving factors in the Koshi River Basin of the Central Himalayas, Nepal. Sustainability 8 (9), 933. https://doi.org/10.3390/su8090933.
Paudel, B., Zhang, Y., Li, S., Liu, L., Wu, X., Khanal, N.R., 2016b. Review of studies on land use and land cover change in Nepal. J. Mt. Sci. 13, 643–660.
Peel, M.C., Finlayson, B.L., McMahon, T.A., 2007. Updated world map of the Köppen-Geiger climate classification. Hydrol. Earth Syst. Sci. 11, 1633–1644.
Polinelli, F.N., 2017. Multitemporal Analysis of Crop Farming in the Dudh Koshi Basin (Nepal) and Climate Change. MS Thesis. Politecnico di Milano 837694. Tutors: M. Gianinetto, D. Bocchiola.
Rai, M., 2007. Climate change and agriculture: a Nepalese case. J. Agric. Environ. 8, 92–95.
Rosenzweig, C., Hillel, D., 1998. Climate Change and the Global Harvest. Oxford University Press, New York.
Rupa Kumar, K., Sahai, A.K., Krishna Kumar, K., Patwardhan, S.K., Mishra, P.K., Revadekar, J.V., Kamala, K., Pant, G.B., 2006. High resolution climate change scenario for India for the 21st century. Curr. Sci. 90 (3), 334–345.
Salerno, F., Guyennon, N., Thakuri, S., Viviano, G., Romano, E., Vuillermoz, E., Cristofanelli, P., Stocchi, P., Agrillo, G., Ma, Y., Tartari, G., 2015. Weak precipitation, warm winters and springs impact glaciers of south slopes of Mt. Everest (central Himalaya) in the last 2 decades (1994–2013). Cryosphere 9 (3), 1229–1247.
Savéan, M., Delclaux, F., Chevallier, P., Wagnon, P., Gonga-Saholiariliva, N., Sharma, R., Neppel, L., Arnaud, Y., 2015. Water budget on the Dudh Koshi River (Nepal): uncertainties on precipitation. J. Hydrol. 531, 850–862.
Schmidhuber, J., Tubiello, F.N., 2007. Global food security under climate change. PNAS 104 (50), 19703–19708.
Schuol, J., Abbaspour, K.C., Yang, H., Srinivasan, R., Zehnder, A.J.B., 2008. Modeling blue and green water availability in Africa. Water Resour. Res. 44, W07406. https://doi.org/10.1029/2007WR006609.
Sharma, M., Dahal, S., 2010. Assessment of impacts of climate change and local adaptation measures in agriculture sector and livelihood of indigenous community in high hills of sankhuwasabha district. In: Understanding Climate Change: Some Case Studies. NAST special edition, Nepal Adaptation of Action (NAPA), Nepal, pp. 16–21.
Shrestha, A.B., Aryal, R., 2011. Climate change in Nepal and its impact on Himalayan glaciers. Reg. Environ. Chang. 11 (1), 65–77.
Sijapati, S., Maskey, S., Timilsina, U., GC, E., Acharya, S., Timilsina, B., et al., 2013. Variability of cropping system and crop production in different agro-ecological zones in the Indrawati River Basin in Nepal. In: Proc. International Conference on Climate Change, Water Resources and Disasters in Mountainous Regions: Building Resilience to Changing Climate. Kathmandu, Nepal.
Soncini, A., Bocchiola, D., Confortola, G., Bianchi, A., Rosso, R., Mayer, C., Lambrecht, A., Palazzi, E., Smiraglia, C., Diolaiuti, G., 2015. Future hydrological regimes in the upper Indus basin: a case study from a high altitude glacierized catchment. J. Hydrometeorol. 16 (1), 306–326.
Soncini, A., Bocchiola, D., Confortola, G., Minora, U., Vuillermoz, E., Salerno, F., Viviano, G., Shrestha, D., Senese, A., Smiraglia, C., Diolaiuti, G., 2016. Future hydrological regimes and glacier cover in the Everest region: the case study of the Dudh Koshi basin. Sci. Total Environ. 565, 1084–1101.
Stevens, B., and other 16 co-authors, 2013. Atmospheric component of the MPI-M Earth System Model: ECHAM6. J. Adv. Model. Earth Syst. 5, 1–27.
Stöckle, C.O., Nelson, R., 1999. Cropping Systems Simulation Model User's Manual. Washington State University. http://www.sipeaa.it/tools/CropSyst/CropSyst_manual.pdf.
Stöckle, C.O., Williams, J.R., Rosenberg, N.J., Jones, C.A., 1992. A method for estimating the direct and climatic effects of rising atmospheric carbon dioxide on growth and yield of crops: part I. Modification of the EPIC model for climate change analysis. Agric. Syst. 38, 225–238.
Stöckle, C.O., Martin, S., Campbell, G.S., 1994. Cropsyst, a cropping systems model: water/nitrogen budgets and crop yield. Agric. Syst. 46 (3), 335–359.
Stöckle, C., Donatelli, M., Roger, N., 2003. CropSyst, a cropping systems simulation model. Eur. J. Agron. 18, 289–307.
Strzepek, K., Boehlert, B., 2010. Competition for water for the food system. Philos. Trans. R. Soc. B. Biol. Sci. 365 (1554), 2927–2940.
Supit, I., van Diepen, C.A., de Wit, A.J.W., Kabat, P., Baruth, B., Ludwig, F., 2010. Recent changes in the climatic yield potential of various crops in Europe. Agric. Syst. 103, 683–694.
Tanner, C.B., Sinclair, T.R., 1983. Efficient water use in crop production: research or research? In: Taylor, H.M., Jordan, W.A., Sinclair, T.R. (Eds.), Limitations to Efficient Water Use in Crop Production. American Society of Agronomy, Madison, Wisc., pp. 1–27.
Torriani, D., Calanca, P., Lips, M., Amman, H., Beniston, M., Fuhrer, J., 2007. Regional assessment of climate change impacts on maize productivity and associated production risk in Switzerland. Reg. Environ. Chang. 7, 209–221.
Tubiello, F.N., Donatelli, M., Rosenzweig, C., Stockle, C., 2000. Effects of climate change and elevated CO2 on cropping systems: model predictions at two Italian sites. Eur. J. Agron. 13, 179–189.
World Bank, 2012. Data Bank. World Development Indicators. Data by country, Nepal Available at: http://databank.worldbank.org/data/views/reports/tableview.aspx.
WWF, World Wildlife Fund, Nepal, 2012. Water Poverty of Indrawati Basin, Analysis and Mapping, June 2012. http://awsassets.panda.org/downloads/water_poverty_book.pdf.